

BRILLIANT PEBBLES: A METHOD FOR DETECTION OF VERY LARGE INTERSTELLAR GRAINS

ARISTOTLE SOCRATES^{1,2} AND BRUCE T. DRAINE^{2,1}

Draft version August 9, 2018

ABSTRACT

A photon of wavelength $\lambda \sim 1 \mu\text{m}$ interacting with a dust grain of radius $a_p \sim 1\text{mm}$ (a “pebble”) undergoes scattering in the forward direction, largely within a small characteristic diffraction angle $\theta_s \sim \lambda/a_p \sim 100''$. Though mm-size dust grains contribute negligibly to the interstellar medium’s visual extinction, the signal they produce in scattered light may be detectable, especially for variable sources. Observations of light scattered at small angles allows for the direct measurement of the large grain population; variable sources can also yield tomographic information of the interstellar medium’s mass distribution. The ability to detect brilliant pebble halos require a careful understanding of the instrument PSF.

Subject headings: dust scattering

1. INTRODUCTION

The size distribution of dust in the diffuse interstellar medium has traditionally been studied through the wavelength dependence of interstellar extinction and polarization, and observations of scattered light from reflection nebulae (cf. Draine 2003). These studies have resulted in models (Weingartner & Draine 2001; Zubko et al. 2004; Draine & Fraisse 2009). where the bulk of the dust mass resides in grains with radii $a \lesssim 0.5 \mu\text{m}$, with approximately 50% of the grain mass above and below a characteristic radius $\sim 0.15 \mu\text{m}$. To account for the observed extinction, these models tend to consume the bulk of available elements such as Mg, Si, and Fe in the “observed” grain population with $a \lesssim 0.5 \mu\text{m}$. Little is known regarding the dust grain size distribution above a grain size of order $\sim 0.5 \mu\text{m}$, aside from the general expectation that grains above this size should contain at most a small fraction of the total dust mass.

Therefore, it was surprising when impact detectors on *Ulysses* and *Galileo* measured a flux of dust particles entering the heliosphere (Landgraf et al. 2000; Krüger et al. 2007) that appeared to indicate that the interstellar grain size distribution extended to much larger grains, with approximately equal mass per unit logarithmic interval out to the largest sizes ($a \approx 1 \mu\text{m}$) that could be detected. This finding was completely at odds with the conclusions drawn from studies of interstellar extinction. Draine (2009) argued that the size distribution inferred for the dust particles approaching the heliosphere could not characterize average interstellar dust, but the situation remains unclear. It is further confounded by radar detection of $a \approx 30 \mu\text{m}$ particles entering the Earth’s atmosphere on solar-hyperbolic trajectories (Taylor et al. 1996; Baggaley 2000, 2004) implying that they are arriving from interstellar space. The mass flux in these particles exceeds the mass flux in $0.2 < a < 1 \mu\text{m}$ particles inferred from the *Ulysses* and *Galileo* observations. If these particles are truly entering

the solar system from interstellar space, it implies a total mass density in $a \gtrsim 0.5 \mu\text{m}$ grains that, at least locally, exceeds that in the $a \lesssim 0.5 \mu\text{m}$ grains in conventional models for interstellar grains. Such an abundance of very large grains would be difficult to understand given the limitations of interstellar abundances of elements from which such grains would be constituted.

In this *Letter*, we show that very large interstellar grains, or “pebbles,” are detectable in scattered light, a phenomenon we refer to as “brilliant pebbles.” The basic idea is presented in §2. Then, in §3 we assess the observability of these scattered light halos, and show that detection is possible even if only a few percent of the interstellar grain mass is in mm-sized particles. Variable sources (e.g., gamma-ray bursts) are particularly useful. In §4 we discuss scattering by a distribution of pebble sizes. We summarize our results in §5.

2. BASIC IDEA

Here we show that small angle scattering of optical photons by large dust grains – “brilliant pebbles” – provides a direct method of determining the size distribution of very large dust grains, and can also provide information on the spatial distribution of the dust.

Particles with radii a large compared to the wavelength λ have total extinction cross sections equal to twice the geometric area (the so-called “extinction paradox” – see, e.g., Bohren & Huffman 1983); 50% of the extinction is contributed by diffraction of light, with much of the energy concentrated in a forward scattering lobe. The characteristic angular radius for the scattering is

$$\theta_0 \approx \frac{\lambda}{\pi a} = 29'' \left(\frac{\lambda}{0.44 \mu\text{m}} \right) \left(\frac{1 \text{ mm}}{a} \right) . \quad (1)$$

For small scattering angles θ_s , the differential scattering cross section $dC_{\text{sca}}/d\Omega \approx \text{constant}$, and for large angles $dC_{\text{sca}}/d\Omega \propto \theta_s^{-3}$. It can be approximated by

$$\frac{dC_{\text{sca}}}{d\Omega} \approx \frac{\pi a^2 / \pi \theta_0^2}{1 + (1.8 \theta_s / \theta_0)^3} . \quad (2)$$

Figure 1 shows exact results for $dC_{\text{sca}}/d\Omega$ calculated for spheres using Mie theory (Mie 1908; Bohren & Huffman 1983). Results are shown for radii

¹ Institute for Advanced Study, Einstein Drive, Princeton, NJ 08540

² Department of Astrophysical Sciences, Princeton University, Peyton Hall-Ivy Lane, Princeton, NJ 08544; socrates@ias.edu; draine@astro.princeton.edu

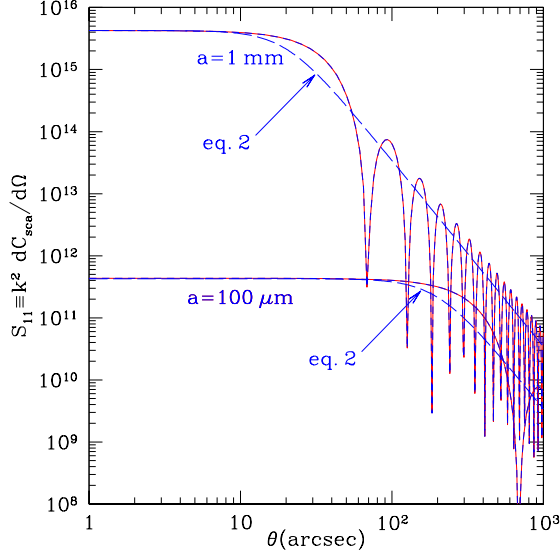


FIG. 1.— Differential scattering cross section vs. scattering angle for photons of wavelength $\lambda = 0.55 \mu\text{m}$ and spheres of radii $a = 100 \mu\text{m}$ and 1 mm . The central lobe dominates the scattering power in both cases. The results are insensitive to composition: the figure actually shows results for both amorphous silicate spheres and graphite spheres, but the curves fall on top of one another. Also shown is eq. (2), which is seen to provide a very good approximation to the overall distribution of scattered power.

$a = 100 \mu\text{m}$ and 1 mm . Eq. (2) provides a good approximation to the scattering for single spheres if one smoothes over the maxima and minima in the diffraction pattern.

Assume that “pebbles” of radius a_p account for a fraction \mathcal{F}_p of the integrated local mass density of dust ρ_d where

$$\rho_d = \frac{4\pi\rho_0}{3} \int_0^\infty da a^3 \frac{dn}{da} \quad , \quad (3)$$

$$\mathcal{F}_p \simeq \frac{a_p^4 (dn/da)_p}{a_{\text{char}}^4 (dn/da)_{\text{char}}} \quad . \quad (4)$$

Here, ρ_0 is the density within a grain, and $a_{\text{char}} \approx 0.15 \mu\text{m}$ is the characteristic dust grain radius that is responsible for most of the dust mass *and* the bulk of the visual extinction in the Galaxy’s interstellar medium. Along any given sight line, the ratio of visual optical depth of pebbles (with radius a_p , and number $\sim a_p (dn/da)_p$) to that of the entire grain population is given by

$$\frac{\Delta\tau_V(a_p)}{\tau_V} \simeq \left(\frac{a_{\text{char}}}{a_p} \right) \mathcal{F}_p \ll 1. \quad (5)$$

Therefore such pebbles, if present, contribute negligibly to interstellar extinction.

Now imagine a point source, that could be variable, as depicted in Figure 2, with an apparent visual magnitude m_V , located at a distance D_0 from an observer. Furthermore, assume that at distance D_p from the observer there is a thin intervening dusty screen of large angular extent contributing a visual extinction A_V .³ Scattering by the pebbles will produce a halo around the source

³ GRB 050724’s time-dependent X-ray halo shows that interstellar dust toward this source is distributed in thin sheets (Vaughan et al. 2006).

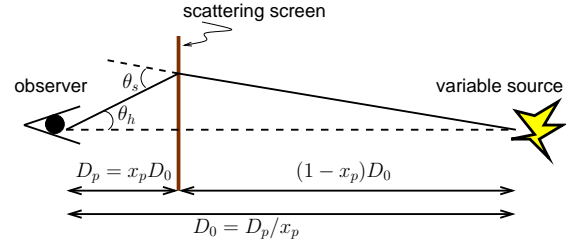


FIG. 2.— Geometry of optical light scattering by pebbles embedded in a dusty scattering screen. Examples of the variable source are novae, variable stars and GRB optical afterglows.

with halo angle $\theta_h \approx (1 - x_p)\theta_s$, where $x_p \equiv D_p/D_0$; the characteristic halo angle is $(1 - x_p)\theta_0$. The time delay Δt_S due to small angle scattering is

$$\begin{aligned} \Delta t_S &\simeq \frac{1}{1 - x_p} \frac{D_p \theta_h^2}{2c} \\ &\simeq \frac{1.2 \times 10^4 \text{ s}}{1 - x_p} \left(\frac{D_p}{1 \text{ kpc}} \right) \left(\frac{\theta_h}{100''} \right)^2 . \end{aligned} \quad (6)$$

With the help of eq. (5), the photon flux scattered by pebbles of size a_p is

$$\begin{aligned} F_S(t + \Delta t_S) &\simeq F_0(t) \left(\frac{a_{\text{char}}}{a_p} \right) \mathcal{F}_p \tau_V \\ &\simeq 10^{-5} F_0(t) \left(\frac{a_{\text{char}}/a_p}{10^{-3}} \right) \left(\frac{\mathcal{F}_p}{10^{-2}} \right) \left(\frac{\tau_V}{1} \right) . \end{aligned} \quad (7)$$

Note that in the above expression, $F_0(t)$ is the “direct” photon power intercepted by the detector and $F_S(t + \Delta t_S)$ is the photon power that underwent small-angle scattering off of pebbles, integrated over a scattering halo with radius $\theta_h \approx (1 - x_p)\theta_s$ with surface brightness

$$\begin{aligned} \frac{\mu_{\lambda,S}(t + \Delta t_S)}{\text{mag arcsec}^{-2}} &\simeq m_\lambda(t) - \\ &2.5 \left[\log \left(\frac{F_S(t + \Delta t_S) (\text{arc sec})^2}{\pi F_0(t) (1 - x_p)^2 \theta_0^2} \right) \right] \end{aligned} \quad (8)$$

where $m_\lambda(t)$ is the apparent magnitude of the point source. The solid angle $\Delta\Omega_h = \pi\theta_h^2 \simeq \pi\theta_0^2 (1 - x_p)^2$ of the scattering halo depends upon the size of the pebbles responsible for the small-angle scattering. With the help of eq. (7), we note that

$$\frac{F_S(t + \Delta t_S)}{F_0(t) \pi \theta_h^2} \approx \frac{\pi \tau_V \mathcal{F}_p}{(1 - x_p)^2} \left(\frac{a_p a_{\text{char}}}{\lambda^2} \right) \quad . \quad (9)$$

Somewhat counter-intuitively, for fixed mass fraction \mathcal{F}_p the halo surface brightness *increases* with increasing pebble size a_p . Even though the total power in scattered light goes as $F_S \propto a_p^{-1}$, the intensity increases $\propto a_p$ because the solid angle that the halo subtends decreases as a_p^{-2} .

3. ASTROPHYSICAL APPLICATIONS AND FEASIBILITY OF DETECTION

In the extreme event that the mass fraction of pebbles is large such that $\mathcal{F}_p \sim \mathcal{O}(1)$, the scattered halo produced by brilliant pebbles is still quite faint. By taking an extreme value of $\mathcal{F}_p \sim 1$ in eq. (7), we see that the

total power scattered is small such that $F_S(t + \Delta t_S) \sim 10^{-3} F_0(t)$.

From Figure 1 we have $\theta = (1 - x_p)\theta_s$. Then, for dust in a single screen (i.e., single time delay for given halo angle θ), the surface brightness of the halo core is

$$\frac{\mu_{\lambda, \max}(t + \Delta t_s)}{\text{mag arcsec}^{-2}} \approx \left[m_\lambda(t) + 19.9 - 2.5 \log \left(\frac{\tau_V \mathcal{F}_p}{(1 - x_p)^2} \frac{a_p}{\text{mm}} \left(\frac{\mu\text{m}}{\lambda} \right)^2 \right) \right] \quad (10)$$

Of course, the above expression is independent of time for a source that does not vary.

3.1. Strategy and Feasibility for Detection

How does one detect a faint – possibly time variable – halo?

For $a_p \sim 1$ mm pebbles, the scattering halo is tens of arc seconds in radius. Dalcanton & Bernstein (2000) obtained accurate surface photometry in the B -band – where the sky is the most dim – of features as faint as 30 mag arcsec $^{-2}$ on scales larger than 10", using exposure times of 45 minutes on a 2.5m telescope. At a dark site, the limiting B surface brightness (for S/N=1) for a $\sim 10''$ region will be

$$\frac{\Delta\mu_{\text{flat}}}{\text{mag arcsec}^{-2}} \approx 29.5 + 2.5 \log_{10}(D/2.5 \text{ m}) + 1.25 \log_{10}(T/45 \text{ min}) \quad (11)$$

Thus $\Delta\mu_{\text{flat}} \approx 31$ mag arcsec $^{-2}$ could be achieved with a 1 hr exposure on an 8 m telescope. The limiting factor will not be sky subtraction, but rather subtraction of the telescope PSF.

The PSF of an optical telescope is typically characterized by a Gaussian “core” produced by atmospheric turbulence, a θ^{-3} halo resulting from diffraction by the large-scale telescope structure (e.g., aperture) at intermediate angles, followed by a “aureole”, varying roughly as θ^{-2} , due to a spectrum of small-scale imperfections (e.g., microripples and dust on the mirrors) (King 1971; Racine 1996; Bernstein 2007).

The PSF of the Dupont 2.5m telescope at Las Campanas was measured by Bernstein (2007) in 2000 September (~ 2 months after mirror realuminization) and can be approximately described at large angular radii by the following broken power law

$$\mu_{\text{psf}} \approx m + 17 + 7.5 \log_{10}(\theta/40'') \quad 6'' < \theta < 40'' \quad (12)$$

$$\approx m + 17 + 5.0 \log_{10}(\theta/40'') \quad 40'' < \theta \lesssim 200'' \quad (13)$$

where μ_{psf} is in mag arcsec $^{-2}$. From here on, we use this exemplary PSF in our estimates.

To estimate exposure times, assume that uncertainties in the sky brightness on 10" scales from an exposure time T_{sky} is given by

$$\frac{\Delta I_{\text{sky}}}{I_{\text{sky}}} = C \left(\frac{1}{I_{\text{sky}} T_{\text{sky}}} \right)^{1/2} \quad (14)$$

where C is a constant. Then, on 10" scales, for an exposure time T_{psf} , the uncertainty in the psf intensity at some angle θ will be given by

$$\frac{\Delta I_{\text{psf}}}{I_{\text{psf}} + I_{\text{sky}}} = C \left(\frac{1}{(I_{\text{psf}} + I_{\text{sky}}) T_{\text{psf}}} \right)^{1/2} \quad (15)$$

Setting $\Delta I_{\text{psf}} = I_{\text{p.h.}}/(S/N)$, we can estimate the required exposure time:

$$T_{\text{psf}} = T_{\text{sky}} (S/N)^2 \left(\frac{\Delta I_{\text{sky}}}{I_{\text{p.h.}}} \right)^2 \left(\frac{I_{\text{psf}} + I_{\text{sky}}}{I_{\text{sky}}} \right) \approx T_{\text{sky}} (S/N)^2 10^{[0.8(\mu_{\text{p.h.}} - \Delta\mu_{\text{sky}}) - 0.4(\mu_{\text{psf}} - \mu_{\text{sky}})]} \quad (16)$$

where we assume $I_{\text{psf}} \gg I_{\text{sky}}$. Dalcanton & Bernstein (2000, 2002) obtained $\Delta\mu_{\text{sky}} = 29.5$ mag arcsec $^{-2}$ for $\mu_{\text{sky}} = 22.2$ mag arcsec $^{-2}$ with $T_{\text{sky}} = 45$ min on the Dupont 2.5 m. Thus, if D is the telescope aperture,

$$T_{\text{psf}} = 0.75 \text{ hr} \left(\frac{2.5 \text{ m}}{D} \right)^2 (S/N)^2 10^{0.8\mu_{\text{p.h.}} - 0.4\mu_{\text{psf}} - 14.72} \quad (18)$$

is the exposure time necessary to detect the pebble halo with signal-to-noise ratio S/N , assuming prior knowledge of the telescope psf.

We now assess the detectability of pebble halos. We set $a_p = 1$ mm, $\mathcal{F}_p = 0.1$, $\lambda = 0.44 \mu\text{m}$, $x_p = 0.5$, and $\tau_V = 1$ in following estimates. The characteristic scattering angle $\theta_0 = 29''$, resulting in a scattered halo with nearly constant surface brightness out to $\theta_h = 14.5''$, with (from eq. 10)

$$\mu_{\text{p.h.}} = (m + 19.11) \text{ mag arcsec}^{-2} \quad (19)$$

For the psf given by eq. (12,13), at $\theta = 14.5''$, a steady source has

$$\mu_{\text{psf}} = (m + 13.69) \text{ mag arcsec}^{-2}. \quad (20)$$

3.2. Statistical Detection

The column density of large dust grains may be correlated with the column density of the sub- μm grains that produce interstellar reddening. It follows that a statistical search for brilliant pebble halos using large-scale imaging, such as the Sloan Digital Sky Survey, may be fruitful. Rather than fit for only an “intrinsic” PSF $P_0(\theta, \phi)$ that is the same for every star in a field (or at most dependent only on position within the field of view), one could determine whether the actual images (excluding regions with small-scale nebular emission) can be better reproduced using a stellar PSF $P_0(\theta, \phi) + E(B - V)P_1(\theta)$, where

$$P_1(\theta_h) = \frac{1}{E(B - V)} \int_0^1 dx_p \frac{f(x_p)}{(1 - x_p)^2} \left(\frac{d\tau_{\text{sca}}}{d\Omega} \right)_{\theta_s} \quad (21)$$

is the dust contribution to the PSF, per unit $E(B - V)$, where $f(x)dx$ is the fraction of the reddening contributed by dust with x_p in $[x, x + dx]$. For a first search, it would be adequate to assume the dust to be halfway to the star (i.e., $f(x) \rightarrow \delta(x - 0.5)$). Using a large number of stars to determine $P_1(\theta)$ may allow detection of the “brilliant pebble” phenomenon at levels that might be impossible for single stars.

3.3. Bright Stars

The pebble halo can be detected with reasonable exposure times on individual bright stars. For a star with $A_V \approx 1$ mag and $m_B < 8.5$ mag (so that $\mu_{\text{psf}} < \mu_{\text{sky}}$) eq. (18) becomes

$$\left(\frac{T}{\text{hr}} \right) \approx 0.75 \text{ hr} (S/N)^2 \left(\frac{2.5 \text{ m}}{D} \right)^2 10^{0.4m_B - 4.91} \quad (22)$$

Thus an exposure time of only 1.4 minutes would suffice for detection (with $S/N = 5$) of the pebble halo around a star with $m_B = 5$ mag. The challenge will be to know the telescope psf well enough to accurately subtract it. This can be accomplished by measuring the psf using stars with minimal reddening. Because the uncertainty in the psf should be small compared to $I_{p.h.}/I_{psf} \approx 0.007(A_V/\text{mag})$, determination of the psf will require care.

3.4. GRB Optical Afterglows and Other Bright Transients

If the source is variable, the ability to detect a brilliant pebble halo of scattered light may increase dramatically. If the PSF of the telescope and atmosphere is stable and known, then point sources whose angular positions are fixed can be subtracted from each successive exposure. In doing so, the pebble halo, which varies in both time and space, may be isolated from the persistent stellar and interstellar background light.

Gamma-Ray bursts (GRBs) occur at a rate \sim once per day in the Universe. Some GRB afterglows have optical luminosities that can compete with those of quasars. For example GRB 990123 reached a peak optical flux slightly brighter than $m_V = 9$ mag (Akerlof et al. 1999), and GRB 080319B had $m_V < 6$ mag for ~ 40 sec (Bloom et al. 2008). There may also be other very bright optical transients: e.g., Shamir & Nemiroff (2006) observed what appeared to be a 5th magnitude flash that lasted ~ 10 min. In the event that a burst with $m_B = 5$ mag were to occur at low Galactic latitudes, the rapid fading of the point source provides the ideal circumstance for detection of a pebble halo, because observation of the time-delayed scattered-light halo can be done without interference from the telescope psf. If an optical transient shone with $m_B = 5$ for a few minutes and then faded, the time-delayed scattered light ‘‘halo’’ (with $\mu = 24.1$ mag arcsec $^{-2}$ if dust with $A_V = 1$ is present in a thin sheet) could be detected in ~ 2 min of integration on an 8 m class telescope.

3.5. Variable Stars

There are several thousand variable stars in the Milky Way brighter than $m_V = 10$ (Paczynski et al. 2006). In fact, from the *ASAS* catalogue, there are over 400 eclipsing binaries with periods shorter than 1 day and $V < 10$. For $\sim 100\mu\text{m}$ pebbles the delay timescale is in terms of hours, rather than tens of minutes. It therefore follows that the pebble halo can be detected by image subtraction if the binary is significantly reddened and distant, if $\sim 100\mu\text{m}$ grains are sufficiently numerous.

4. SMALL ANGLE SCATTERING FROM A SIZE DISTRIBUTION OF PEBBLES

So far, we have considered small angle scattering due to the presence of pebbles of a single characteristic size. Now, we briefly consider a distribution of sizes. For simplicity, we assume that the pebble size distribution resembles a power law

$$\frac{dN}{da} = \mathcal{N}a^{-p} \quad a_{\min} < a < a_{\max} \quad (23)$$

where $N(a)$ is the column density of pebbles with radii $a_p < a$. For $p = 4$ (i.e., equal mass per logarithmic

interval in a_p) the normalization constant is given by

$$\mathcal{N} \approx \frac{\tau_V}{2\pi \ln(a_{\max}/a_{\min})} \mathcal{F}_p \quad (24)$$

where the optical depth τ_V is assumed to be provided by the dominant dust population with radii $a_{\text{char}} \approx 0.15\mu\text{m}$, with extinction cross sections $C_{\text{ext}} \approx \pi a_{\text{char}}^2$.

For scattering by material in one scattering screen, we define the differential scattering optical depth such that, at halo angle θ_h , the scattered intensity is

$$I(\theta_h, t + \Delta t_s) = \frac{F_0(t)}{(1-x_p)^2} \left(\frac{d\tau_{\text{sca}}}{d\Omega} \right)_{\theta_h} \quad (25)$$

where

$$\left(\frac{d\tau_{\text{sca}}}{d\Omega} \right)_{\theta_h} = \int da \left(\frac{dN}{da} \right) \left(\frac{dC_{\text{sca}}}{d\Omega} \right)_{\theta_s = \theta_h/(1-x_p)} \quad (26)$$

With the help of the approximation (2) for $dC_{\text{sca}}/d\Omega$, the differential scattering optical depth is

$$\frac{d\tau_{\text{sca}}}{d\Omega} \simeq \mathcal{N} \frac{\pi^2}{\lambda^2} \int_{a_{\min}}^{a_{\max}} \frac{a^{4-p} da}{1 + (a/a_c)^3} \quad (27)$$

$$a_c \equiv \frac{(1-x_p)\lambda}{1.8\pi\theta_h} \quad (28)$$

We can distinguish three regimes: the core, with $\theta_h < \theta_1 \equiv (1-x_p)\lambda/1.8\pi a_{\max}$; the intermediate halo, with $\theta_1 < \theta_h < \theta_2 \equiv (1-x_p)\lambda/1.8\pi a_{\min}$; and the outer halo, with $\theta_h > \theta_2$. For $2 < p < 5$ we have

$$\frac{d\tau_{\text{sca}}}{d\Omega} \approx \mathcal{N} \frac{\pi^2 a_{\max}}{\lambda^2} \quad \text{for } \theta_h \ll \theta_1 \quad (29)$$

$$\approx \mathcal{N} \frac{2\pi^2(1-x_p)^{5-p}}{(5-p)(p-2)(1.8\pi)^{5-p}} \frac{1}{\lambda^{p-3}} \frac{1}{\theta_h^{5-p}} \quad \text{for } \theta_1 \ll \theta_h \ll \theta_2 \quad (30)$$

$$\approx \mathcal{N} \frac{\pi^2(1-x_p)^3}{(p-2)(1.8\pi)^3 a_{\min}^{p-2}} \frac{\lambda}{\theta_h^3} \quad \text{for } \theta_h \gg \theta_2 \quad (31)$$

In Figure 3, we perform the integral in eq. (27) over a $p = 4$ pebble size distribution for $\lambda = 0.4405\mu\text{m}$ and $0.802\mu\text{m}$. As an illustrative example, consider the case in Figure 3 where the large pebble size cutoff $a_{\max} = 1.0$ cm for $\lambda = 0.4405\mu\text{m}$. The angle θ_1 marking the transition from the core, where $d\tau_s/d\Omega \approx \text{const}$, to the intermediate halo, where $d\tau_s/d\Omega \propto \theta_h^{5-p}$, indicates the value of the upper cutoff in pebble size, $a_{\max} \approx (1-x_p)\lambda/1.8\pi\theta_1$.

The power-law index p for the size distribution can be determined from both the angular dependence θ_h^{p-5} and the color ($d\tau_s/d\Omega \propto \lambda^{3-p}$) of the intermediate halo ($\theta_1 \ll \theta_h \ll \theta_2$). The large angle behavior $d\tau_{\text{sca}}/d\Omega \propto \theta^{-3}$ for $\theta \gtrsim \theta_2$ indicates that at these angles, all of the pebble size range $[a_{\min}, a_{\max}]$ is in the large scattering angle regime.

Figure 3 shows how $d\tau_{\text{sca}}/d\Omega$ varies with photon wavelength. For shorter wavelengths, the halo makes the transition from the small angle to intermediate angle regime at smaller angles. The scattered halo will be very blue in the core: for $p = 4$ the core will have a color excess $B - I = -2.5 \log_{10}(0.8020/0.4405)^2 = -1.30$ mag relative to the unscattered source, while the intermediate zone beyond the core will have $B - I = -0.65$ mag. For $\theta > \theta_2$ the halo will be red, with $B - I = +0.65$ mag, but the combination of long delay time Δt_S and low surface brightness may render this outer halo undetectable.

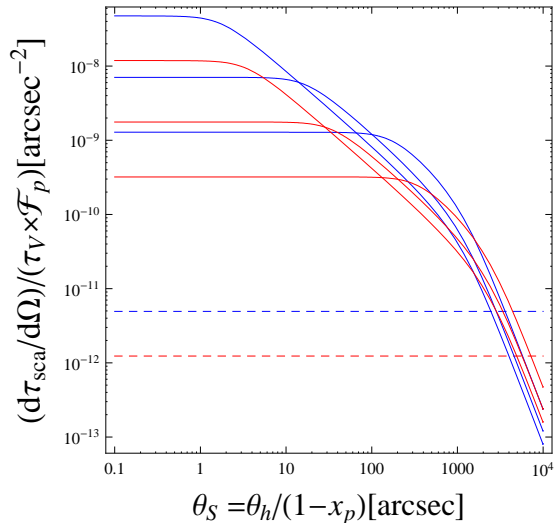


FIG. 3.— Pebble size-averaged differential optical depth $(d\tau_{\text{sca}}/d\Omega)/(\tau_V \mathcal{F}_p)$ vs. scattering angle θ_s for photons of wavelength $\lambda = 0.4405 \mu\text{m}$ (blue) and $\lambda = 0.802 \mu\text{m}$ (red). Each curve represents $dC_{\text{sca}}/d\Omega$, integrated over an a^{-4} pebble size distribution, but with varying ranges in pebble size. The lower limit for pebble sizes $a_{\text{min}} = 10 \mu\text{m}$ for all of the curves. The maximum pebble size $a_{\text{max}} = 1 \text{ cm}$, 1 mm and $10^2 \mu\text{m}$ for the top, middle and bottom curves, respectively, for each of the two photon wavelengths. At small scattering angles, $d\tau_{\text{sca}}/d\Omega \propto a$ constant, while $d\tau_{\text{sca}}/d\Omega \propto \theta_s^{-3}$ at large scattering angles, recovering the asymptotic behavior of eq. (2). At intermediate angles, $d\tau_{\text{sca}}/d\Omega \propto \theta_s^{-1}$. This ‘intermediate’ angle range is more prominent for broad distributions of pebble sizes. The dashed lines at the bottom represent the limit where the pebbles are replaced purely by “normal” $a \simeq 0.15 \mu\text{m}$ grains for each photon band. As long as $\mathcal{F}_p \gtrsim 10^{-2}$ for the pebble-size distributions utilized in this figure, then the variable scattered light should be dominated by pebbles rather than normal dust.

5. SUMMARY

We propose a method for the detection of extremely large ($\sim 0.01 - 1 \text{ cm}$) dust grains. When the ratio of photon wavelength to grain size $\lambda/a \ll 1$, scattering of light is highly peaked in the forward direction, with a characteristic scattering angle $\theta_0 \sim \lambda/\pi a \sim 30(1 \text{ mm}/a_p)''$. For a variable source, the halo will lag with a characteristic time-scale $\sim 10 \text{ min}$ for scattering by 1 mm pebbles

at a distance $\sim 1 \text{ kpc}$. We refer to this phenomena as “brilliant pebbles.”

Detection of the brilliant pebble halo will be technically challenging. Even for favorable assumptions regarding the pebble size distribution, an accurate determination of the telescope PSF is required in order to detect such a low surface brightness signal. Nevertheless, we show that a pebble halo could be detected using existing facilities if the mass in $\sim 1 \text{ mm}$ pebbles is more than a few percent of the total dust mass, as has been suggested by observations of high-velocity dust grains in interplanetary space and hyperbolic micrometeors (see § 1).

Detection is best accomplished using a well-baffled telescope with a freshly aluminized mirror, to minimize scattering by small-scale imperfections such as dust on the mirror.

A brief but bright optical burst would be ideal, as the direct light can fade while the time-delayed pebble halo persists, allowing the telescope PSF and the pebble halo to be separated in the time domain. Also, the pebble halo from a bright short period eclipsing binary that is significantly reddened can be subtracted from the PSF in the time domain as well.

If a “brilliant pebble” halo is detected, the angular variation of the halo intensity will indicate the pebble size range and the form of the particle size distribution. The halo will be very blue in the core, and moderately blue in the intermediate halo; the color of the intermediate halo provides an independent measure of the size distribution. If the source is suitably variable, the distance to the pebbles can be determined from the time delay of the halo relative to the point source.

Upper limits on brilliant pebble halos can provide valuable constraints on the size distribution of solid particles in the interstellar medium.

We thank P. Chang, M. Pan and A. Witt for fruitful discussions and the referee, whose comments improved our paper. AS acknowledges support from a Lyman Spitzer Jr. Fellowship given by Astrophysical Sciences at Princeton U. and a Friends of the Institute Fellowship at IAS, Princeton. BTJ thanks the IAS for hospitality during summer 2008 and support from NSF grant AST-0406883.

REFERENCES

- Akerlof, C., et al. 1999, *Nature*, 398, 400
 Baggaley, W. J. 2000, *J. Geophys. Res.*, 105, 10353
 —. 2004, *Earth Moon and Planets*, 95, 197
 Bernstein, R. A. 2007, *ApJ*, 666, 663
 Bloom, J. S., et al. 2008, *ArXiv e-prints*
 Bohren, C. F., & Huffman, D. R. 1983, *Absorption and Scattering of Light by Small Particles* (New York: Wiley)
 Dalcanton, J. J., & Bernstein, R. A. 2000, *AJ*, 120, 203
 —. 2002, *AJ*, 124, 1328
 Draine, B. T. 2003, *ARA&A*, 41, 241
 —. 2009, *Space Science Reviews*, 143, 333
 Draine, B. T., & Fraisse, A. A. 2009, *ApJ*, 696, 1
 King, I. R. 1971, *PASP*, 83, 199
 Krüger, H., Landgraf, M., Altbelli, N., & Grün, E. 2007, *Space Science Reviews*, 130, 401
 Landgraf, M., Baggaley, W. J., Grün, E., Krüger, H., & Linkert, G. 2000, *J. Geophys. Res.*, 105, 10343
 Mie, G. 1908, *Annalen der Physik*, 330, 377
 Paczyński, B., Szczygiel, D. M., Pilecki, B., & Pojmański, G. 2006, *MNRAS*, 368, 1311
 Racine, R. 1996, *PASP*, 108, 699
 Shamir, L., & Nemiroff, R. J. 2006, *PASP*, 118, 1180
 Taylor, A. D., Baggaley, W. J., & Steel, D. I. 1996, *Nature*, 380, 323
 Vaughan, S., et al. 2006, *ApJ*, 639, 323
 Weingartner, J. C., & Draine, B. T. 2001, *ApJ*, 548, 296
 Zubko, V., Dwek, E., & Arendt, R. G. 2004, *ApJS*, 152, 211